A study of PHENIX's Muon Identifier's efficiency

Report of an internship under the supervision of RIKEN, Wako - Japan

References:
- Caussin Sarah
M2 Noyaux, atomes, collisions
- Ban Gilles
- Nakagawa Itaru
- Année universitaire 2013/2014

ENSICAEN
6, boulevard Maréchal Juin – CS 45 053 – F- 14050 Caen Cedex 4
Tél. +33 (0)2 31 45 27 50
Fax +33 (0)2 31 45 27 60

Table of contents

Acknowledgements

This study could not have been conducted without the help of many people, which is why I feel it is necessary to express my gratitude first and foremost.

I would first like to thank Dr. Itaru Nakagawa for giving me the opportunity to work on this study once more, for helping me through it, and for everything he taught me during this internship. I would also like to extend my thanks to all of RIKEN's staff, not only for their warm welcome, but also for all the help and advice they provided me with.

I would also like to express my gratitude to the ENSICAEN and the Université de Caen Basse-Normandie (UCBN) teaching staff for the quality of their lectures, as they have become the foundation of my knowledge and the tools I used to tackle this study.

This internship was a great experience, and I deeply thank everyone who helped me complete it.

Introduction

As a third-year engineering student at the ENSICAEN and a M2 physics student at the UCBN, I was given the opportunity to work for six months under the supervision of Dr. Nakagawa Itaru in the Radiation Laboratory of RIKEN.

Considering that I have started working in 2013 on PHENIX's Muon Identifier's efficiency during last year's three-month internship, this study acts as a continuation and provides a better understanding as well as a developed analysis of the subject.

In this report I will convey my work during this internship which aim was mainly to study and improve the High Voltage method, one of the two ways used to calculate MuID's efficiency. I will start with a presentation of MuID in order to get to know the detector I have been working with as well as the stakes of my study. I will then offer a detailed explanation of the High Voltage method and compare it with the second method. Finally, I'll provide an improvement of High Voltage method and give some pointers to the next issue to be tackled.

I/ Presentation of MuID

1/ Introducing PHENIX

a. RIKEN and Brookhaven National Laboratory

RIKEN [1], short for Rikagaku Kenkyūsho, is a Japanese research institute founded in 1917 whose main campus is located in Wako, right outside of Tokyo. It conducts research in a large range of fields of science, including physics as well as biology, chemistry or medical science.

Brookhaven National Laboratory [2], known as BNL, is an United States research facility located on the center of Long Island, New York. Like RIKEN, it conducts studies in multiple fields and hosts the Relativistic Heavy Ion Collider [3], RHIC, able work with spin-polarized proton as well as heavy ions.

The Spin Group is a collaboration between researchers affiliated with BNL or RIKEN's Radiation Laboratory where I have been working. The group is currently conducting research on the spin structure of the proton, which has been proven not to be carried exclusively by its quarks by the 1987 EMC experiment [4], through the use of spin-polarized proton-proton collisions at RHIC. These collisions are studied using PHENIX, the **P**ioneering **H**igh **E**nergy **N**uclear **I**nteraction e**X**periment.

b. PHENIX and its muon systems

PHENIX's missions are quite diverse: they include the search of the Quark-Gluon Plasma, the creation of a map of the Quantum Chromodynamics phase diagram, the study of matter under extreme conditions of temperature and pressure, and as previously mentioned the study of the proton's spin.

Being such a pluripotent experiment, PHENIX consists of a dozen sub-system detectors, as seen on Fig. 1, able to track and extract information from different particles for a large number of analysis' purpose.

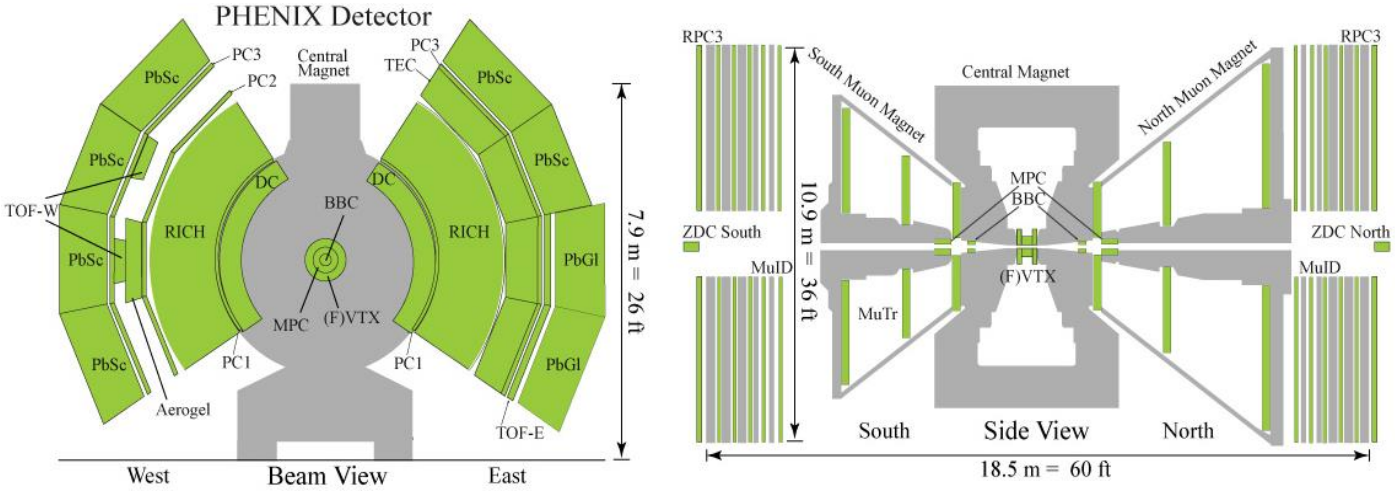

Fig. 1. Front and Side view of PHENIX [5]

As they are trying to measure the sea-quark polarization component of the proton spin, Spin Group is currently conducting research involving the W boson produced in polarized proton-proton collision as a probe:

$$u\bar{d} \rightarrow W^+$$
$$d\bar{u} \rightarrow W^-$$

This W boson decays into a muon, which is the particle of interest from a detection point of view, and an antineutrino:

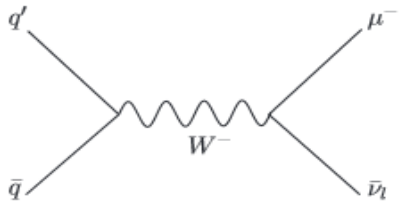

Fig. 2. Feynman diagram for W⁻ production and decay into a muon and an antineutrino

To achieve tracking and identifying of the muon created during such decay, the group has been working with the Muon Tracker (called MuTr Fig.1) and Muon IDentifier (referred as MuID Fig. 1) sub-systems. All muon sub-systems are oriented transversely to the beam line and consist of two semi-symmetric arms, North and South, with the interaction point at their center.

While I have been working with MuID and MuTr in 2013, this year my study has focused entirely on MuID. As the mass of the W boson is 80 GeV/c², it is rarely created in RHIC's 500GeV collisions. To get sufficient data, MuID was operated under very high luminosity. However, MuID's efficiency drops rapidly with high luminosity, meaning it has to be studied carefully.

2/ A deeper look into MuID

a. General view of MuID

For both arms, MuID, circled in red on Fig. 3, lies behind the MuTr sub-system with a 30 cm thick steel plate between them. One MuID arm consists of five detection layers (red on Fig. 3) alternated with four steel absorber plates (grey on Fig. 3).

These absorbers are used to stop part of the hadrons that are able to go through the first absorber plate (grey on Fig. 3) and have thicknesses that vary from 10 cm for the first to ones to 20 cm for the last two ones. Before the blue plate, in grey on Fig. 3 is the last absorber plate, which is used to shield the detection layers from the background particles coming from the beam line.

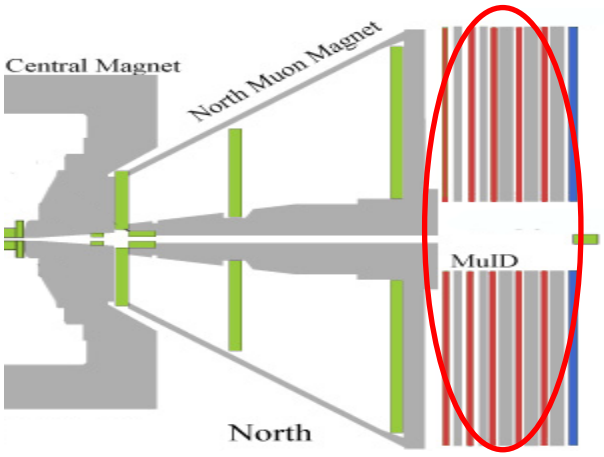

Fig. 3. Muon system North arm

b. Geometry of MuID's gaps

The five detector layers of MuID are called "gaps" and are divided into six panels distributed around the beam line, as seen on Fig. 4. In order to avoid dead space, adjacent panels overlap each other. Every panel is then filled with two planes of Iarocci tubes [6], one plane having vertically-oriented tubes while the other has horizontally-oriented tubes.

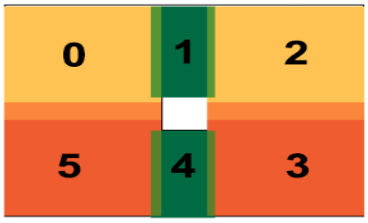

Fig. 4. MuID's gap geometry [7]

The so-called Iarocci tubes are rectangular drift chambers running in streamer mode consisting of 8 anode wires contained in a graphite-coated cathode. The gas used is a mixture of CO_2 and up to 25% of i-C_4H_{10}. This technology has been chosen because it has been proven reliable, long-lived, compact, low cost and easy to obtain.

A large panel (i.e. panels 0, 2, 3 and 5) typically consists of about sixty tubes, while a small one (i.e. panels 1 and 4) consists of around twenty tubes for vertical planes and forty tubes for horizontal ones.

c. MuID's high voltage supplies

In order to minimalize drift time and maximize efficiency, a plane actually consists of two staggered layers of tubes. Two staggered tubes are called a "channel", as seen on Fig. 5.

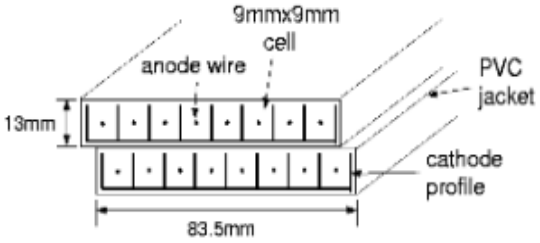

Fig. 5. A MuID channel [7]

The tubes of a channel are supplied by different high voltage supply chains (later referenced as HV chain). Typically, a HV chain serves around twenty tubes, and two HV chains that supply the same channels make a HV "group". On Fig. 6, the HV groups are represented by red, green and grey on their respective panels, and in black are indicated the numbers of the tubes they supply.

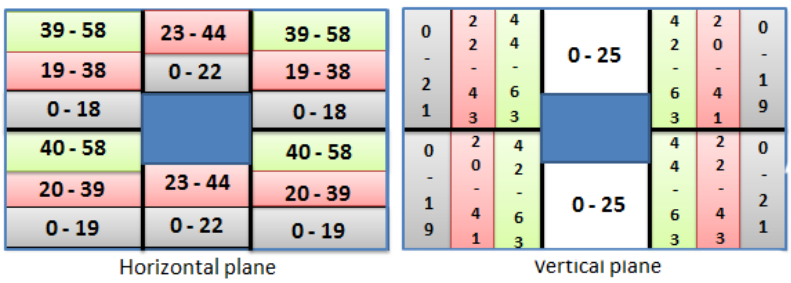

Fig. 6. MuID's HV groups and their tube numbers

II/ Evaluation of MuID's efficiency with the high voltage method

1/ MuID's two efficiency evaluation methods

a. Data-driven method

With the data-driven method (further referred as DD method), efficiency of a given gap is determined using the tracks registered in the previous and next gap. As suggested by Fig. 7, if a signal is recorded in gap *i-1* and *i+1*, then the muon necessarily went through gap *i*.

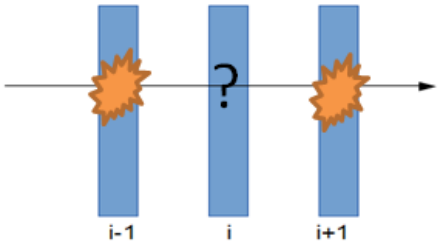

Fig. 7. DD method principle

The efficiency of gap *i* can therefore be evaluated by dividing the number of tracks indeed recorded in gap *i* by the number of tracks recorded both in gap *i-1* and *i+1*. Flaws of this method include the fact that it isn't as reliable for the last gap. Indeed, though the first gap can only rely on the next gaps to reconstruct the road of a muon, additional information is required to know whether or not the muon has been stopped before the last gap.

b. High voltage method

The high voltage method (referred as HV method) calculates the efficiency of a tube using an empirical formula that relies on the current drawn from the supplies by the HV chains:

$$\text{Efficiency} = 0.96(1 - 2.4 \times 10^{-6} \times V_{\text{eff}}^2) \quad (1)$$

Where $\mathbf{V_{eff}}$ is given by:

$$V_{\text{eff}} = V - R \times I_{\text{drawn}} \quad (2)$$

In which **V** is the voltage delivered by the supplies and equals 4400 V**, R** is the resistance of a tube and equals 400 MΩ, and $\mathbf{I_{drawn}}$ is the current drawn by a tube, as seen on Fig. 8.

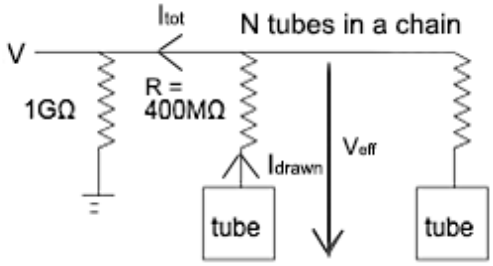

Fig. 8. Simplified circuit diagram of a HV chain

This empirical formula was determined in 2004 by a fit of the V_{eff} vs. Efficiency graph shown on Fig. 9. In this graph, each different color represents a HV group.

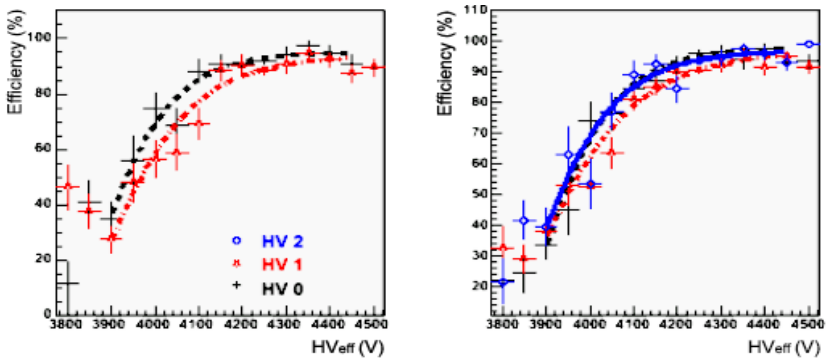

Fig. 9. V_{eff} vs. Efficiency graph for two different panels [8]

In the past, both methods have demonstrated consistent efficiencies, as seen on Fig. 10, which is why HV method has not been used in recent analysis. However, as RHIC is now operating at higher rates, HV method needs to be reevaluated in order to provide a double-check for the DD method.

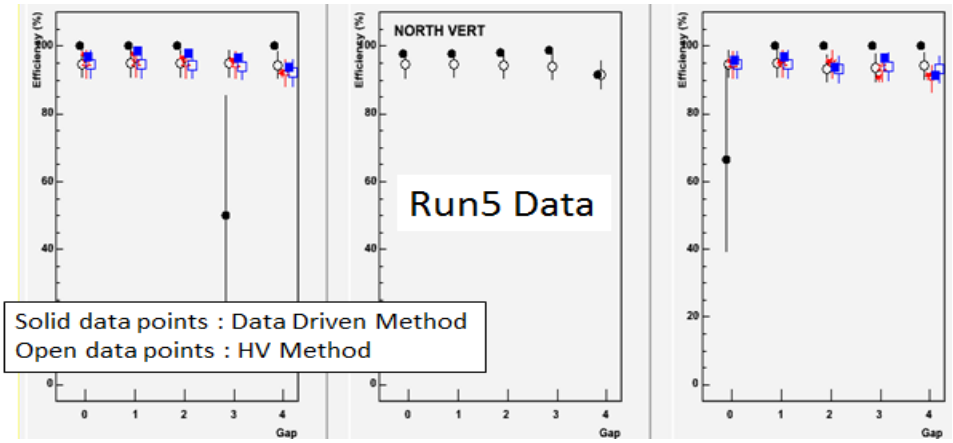

Fig. 10. Efficiency of both methods for the five gaps [8]

I have worked on this analysis last year as a part of my M1 internship, and provided a basic script to evaluate efficiency using the HV method. It has since then been modified by my tutor, Dr. Nakagawa Itaru, and has evolved into a more complicated program.

This year, I have been asked to run a cross-check of the current version of the program by writing my own version of it, and then to conduct a comparison between both methods to determine which corrections should be applied to HV method if they were to disagree.

2/ HV method process

a. Evaluating I_{tot}

The information MuID's database gives us access to is the total raw current drawn by a HV chain, $\boldsymbol{I_{raw}^{tot}}$. Typically, a HV chain supplies around N = 20 tubes. To get the current drawn from the supplies because of the passage of particles coming from the RHIC collisions, $\boldsymbol{I_{tot}}$, we have to subtract the baseline current, $\boldsymbol{I_{baseline}^{tot}}$ from it. $\boldsymbol{I_{baseline}^{tot}}$, is due to the addition of the DC current

drawn when HV is applied, the tube leakage current appearing when the tubes are degraded and the passage of cosmic particles, in order of importance of the contribution.

$$I_{tot} = I_{raw}^{tot} - I_{baseline}^{tot} \quad (3)$$

This baseline current is calculated during so-called cosmic runs during which there are no RHIC collisions. This allows the detectors to measure the background current. On Fig. 11 is the current drawn by a chain during such runs.

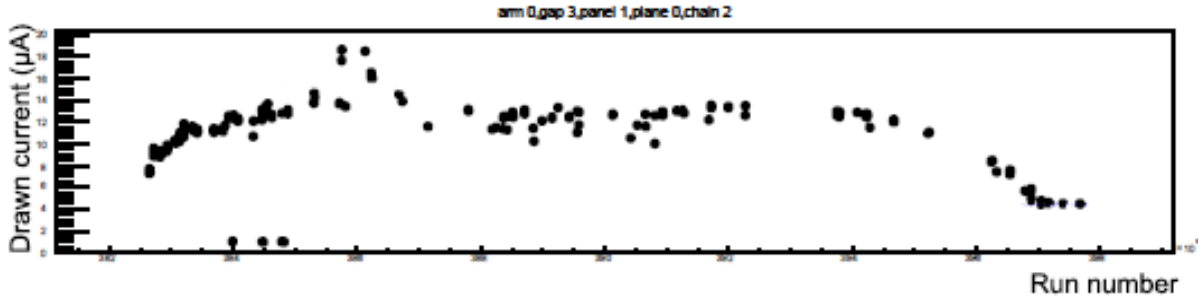

Fig. 11. Current drawn during cosmic runs

In order to evaluate the baseline current during physics runs, it is necessary to interpolate the data taken during cosmic runs. In the previous program, the interpolated points were evaluated by taking the average current between cosmic runs (Fig 12, in green). However I chose to use a linear interpolation (Fig 12, in red) in order to better take into account the fluctuations between two cosmic runs.

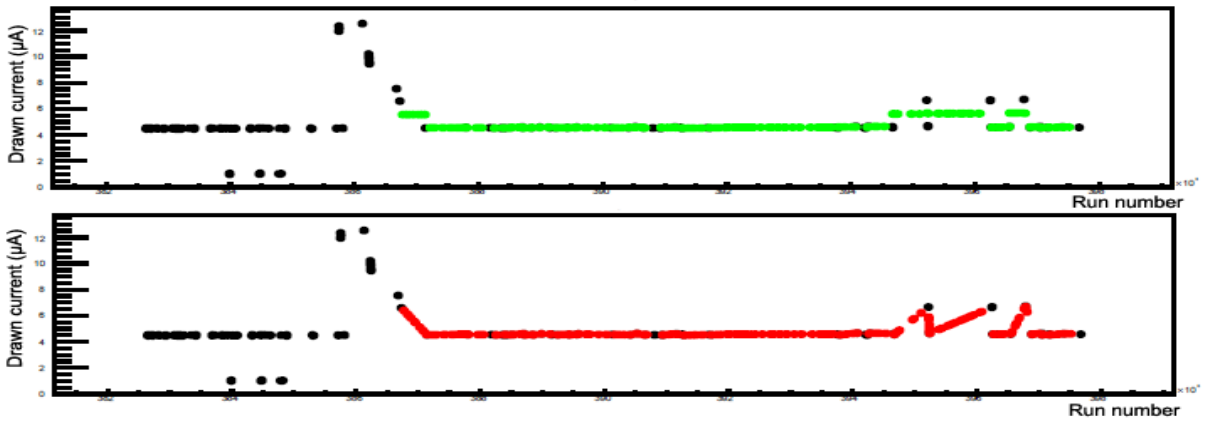

Fig. 12. Difference between the two interpolation methods

b. Evaluating I_{drawn}

Once the total drawn current, I_{tot}, has been evaluated, we have to calculate the current drawn by a single tube in a chain, I_{drawn}. We assumed that all tubes draw the same amount of current; therefore the current drawn by a single tube is given by:

$$I_{drawn} = \frac{I_{tot}}{N_{act}} \quad (4)$$

Where N_{act} is the number of active tubes in a chain.

In normal conditions, $N_{act} = N$, the total number of tubes. However, sometimes anode wires break. To properly take this into account, it is necessary to evaluate N_{bk} the number of broken wires in a chain. N_{act} is then given using:

$$N_{act} = N - N_{bk} \quad (5)$$

N_{bk} can be evaluated using the current drawn during cosmic runs. From Fig. 8 we can write that the overall resistance with N_{bk} broken wires is:

$$R[G\Omega] = \frac{1}{1+\frac{1}{0.4}N_{bk}} \quad (6)$$

Therefore the current drawn with N_{bk} broken wires is:

$$I[\mu A] = \left(1 + \frac{1}{0.4}\,N_{bk}\right) \times V\ \textbf{[kV]} \quad (7)$$

With this formula, we calculated the values in Tab. 1:

$I[\mu A]$	N_{bk}
4.4	0
15.4	1
26.4	2

Tab. 1. Evaluation of the number of broken wires

This allows us to determine the number of broken wires by simply checking the value of the current drawn during cosmic runs.

As seen on Fig. 13, although baseline current behavior is stable for most HV chains, sometimes the current shows unstable behavior thorough all runs. This is the main reason I chose to implement a mathematical method rather than estimating the number of broken wires by eye as it was previously done: using an automatic algorithm provides an equal treatment for all behaviors and is devoid of the human eye bias.

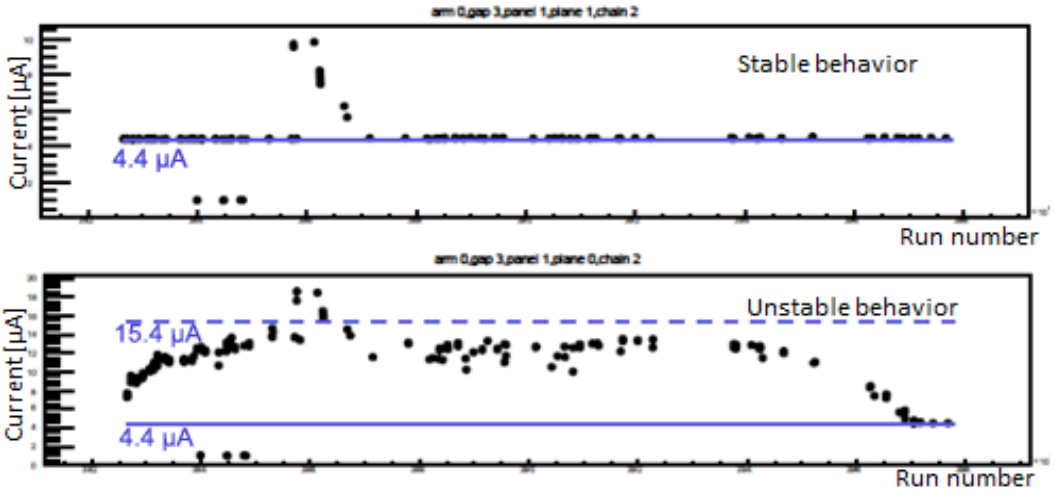

Fig. 13. Examples of stable and unstable baseline behaviors

The first step of this algorithm is to fit the baseline current vs. run number over the period of physics run in order to take into account cases where the wires broke after the physics runs started. Such a case is shown Fig. 14.

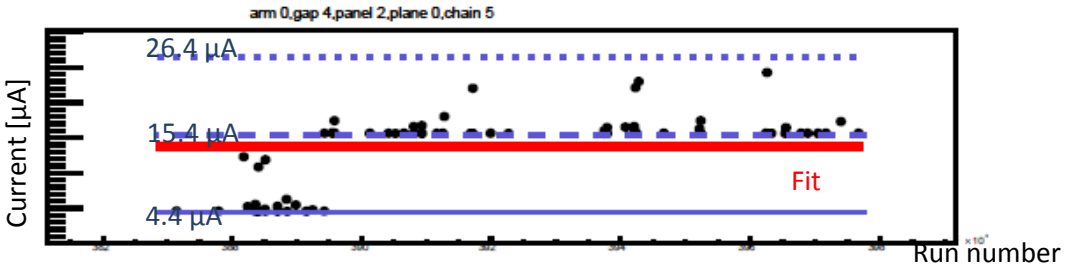

Fig. 14. Example of a wire breaking after the physics runs period started

The algorithm then uses the parameter of the fit to decide the number of broken wires. If the parameter is under $\frac{15.4+4.4}{2} = 9.9\ \mu A$ (green zone, Fig. 15), there is no broken wire; if the parameter is between 9.9µA and $\frac{15.4+26.4}{2} = 20.9\ \mu A$ (blue zone, Fig. 15) there is one broken wire; if the parameter is over 20.9 µA (purple zone, Fig. 15) there are two broken wires.

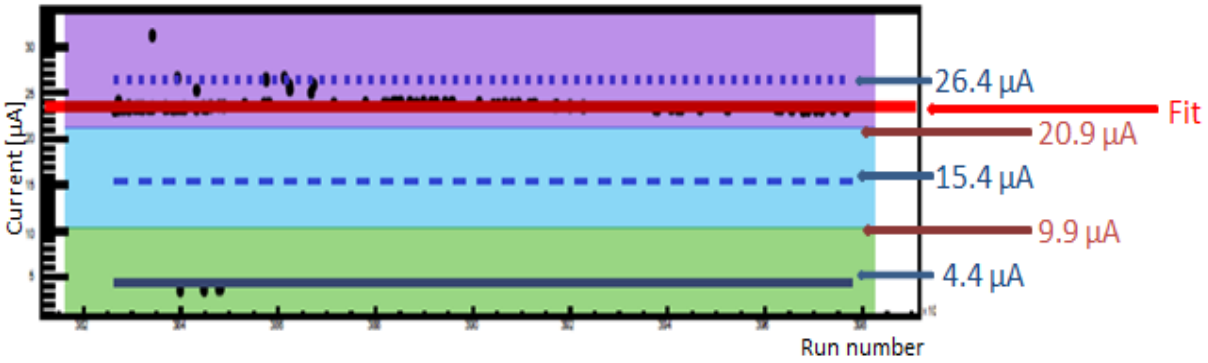

Fig. 15. Illustration of the algorithm's method to decide the number of broken wires

$\mathbf{V_{eff}}$ is then evaluated using the formula (2), which lets us calculate the efficiency **ε** using the formula (1), and then allowing us to compare it with DD method. Documentation on the changes brought by my program is provided in the Appendix 1/.

III/ Comparing the data-driven and high voltage methods

1/ Average deviation

After evaluating both methods, they can be plotted together to be compared:

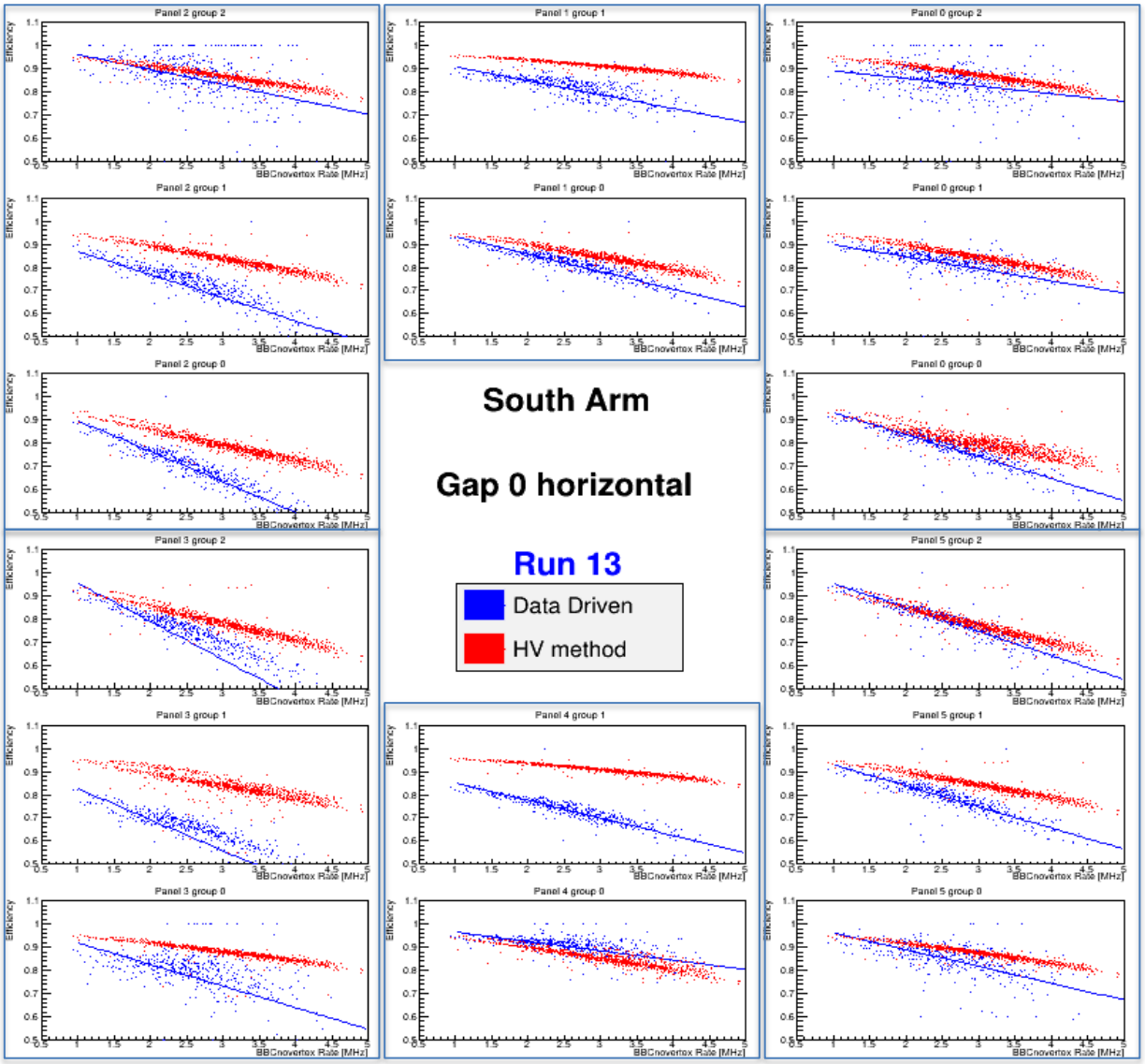

Fig. 16. Efficiency calculated with both methods for South arm, gap 0, horizontal plane
Every graph corresponds to a HV group, panels are boxed in blue
X axis is BBC rate [kHz], corresponding to luminosity and Y axis is efficiency

In most cases the results are not overlapping at all, and even have different luminosity dependency. Also, the data points from the HV method (red) seem to have a tendency (though that's not the case for every group) to have higher values than the ones from the DD method (blue). In order to give a quantitative way to describe this we introduced a new value.

This so-called average deviation between both methods has been defined as:

$$\Delta\varepsilon = \frac{\overline{\varepsilon_{HV}} - \overline{\varepsilon_{DD}}}{\overline{\varepsilon_{HV}}} \quad (9)$$

In which $\overline{\varepsilon_{HV}}$ and $\overline{\varepsilon_{DD}}$ are evaluated for every HV group by using a fit of the Efficiency vs. Luminosity of the beam graph, as shown in Fig. 17a.

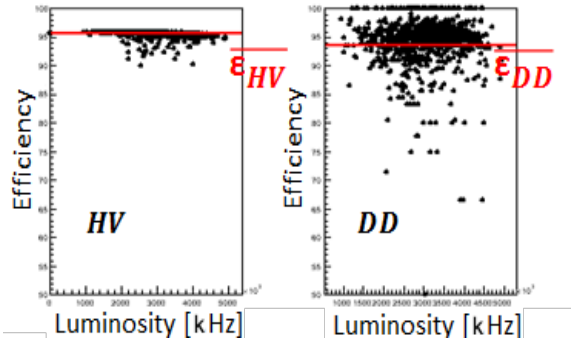

Fig. 17a. Efficiency vs. Luminosity of the beam for both methods

I then built a histogram shown on Fig. 17b to summarize the information:

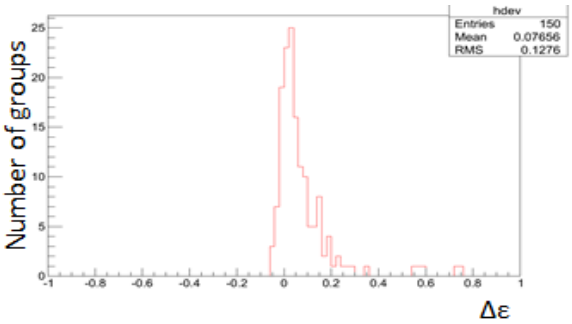

Fig. 17b. Average deviation

This histogram shows us that HV method efficiencies have a tendency to be higher than DD method ones, with the mean of the distribution being about 8%. Also, though most results are consistent within a 20% range, in some cases the inconsistency can go up to 75% and deserve some further investigation, which is the main motivation for the geometry checks that follow.

2/ Group order consistency check

a. Raw group order

As it was previously mentioned, MuID's HV supplies are divided into groups. The group numbering can be seen in Fig. 18:

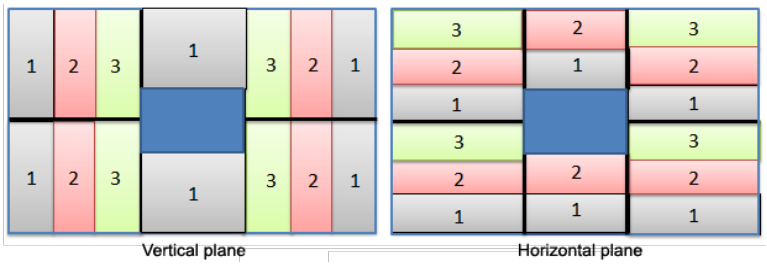

Fig. 18. Group numbering

Since they have greater hit rates, we expect the groups closer to the beam line to have generally lower efficiencies than the ones far away from it.

To check if both methods actually show this, I plotted group efficiencies vs. luminosity of the beam, panel by panel, and fitted these data points with a linear fit, as shown on Fig. 19. As we can see on these graphs, the efficiency indeed decreases when the luminosity raises, and the groups furthest from the beam line do have a better efficiency in most cases.

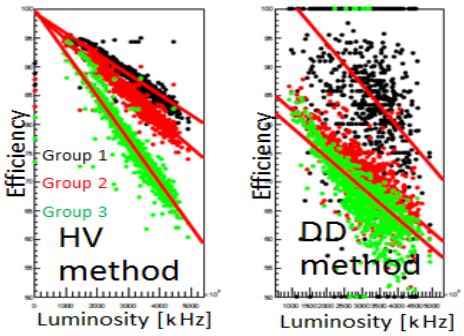

Fig. 19. Normal group order behavior for vertical plane ($\varepsilon_1 > \varepsilon_2 > \varepsilon_3$)

In some cases though, the group order shows unexpected behaviors, such as in Fig. 20 where the efficiency of the beam closest to the beam line has somehow better efficiency than one that is further.

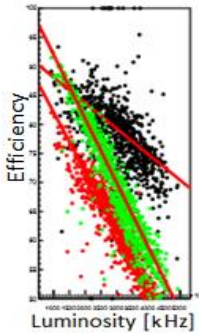

Fig. 20. Odd group order behavior for vertical plane ($\varepsilon_1 > \varepsilon_3 > \varepsilon_2$)

To better study these behaviors, we classified the different group orders into three categories:

- The expected order in which efficiency is decreasing when the group gets closer to the beam line, as shown on Fig. 19;
- The halfway order in which two of the three groups of a panel are reversed, much like the panel shown Fig. 20 (when group order is reversed in panels 1 and 5 that only have two groups, they are counted as halfway order);
- The unexpected order all three groups of a panel are in reversed order.

To get a better view of the occurrence of odd cases, I programmed a script to determine the group order for every panel. However, as it has been pointed out to me, though the group order is quite obvious in most circumstances, sometimes the efficiency distributions overlap each other, as shown in Fig. 21.

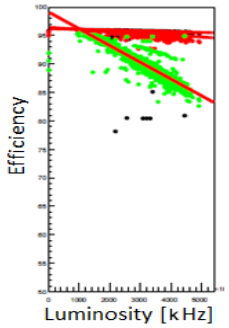

Fig. 21. Example of overlapping efficiency distributions

b. Seriousness

In order to solve that problem, we introduced a weight to measure how relevant each panel is. This "seriousness", as we called it, takes into account both the spreading of the efficiency distributions and the distance between the different group distributions.

The seriousness is given the following formula:

$$S = \frac{|\Delta_{12}|}{\sigma_1 + \sigma_2} + \frac{|\Delta_{23}|}{\sigma_3 + \sigma_2} + \frac{|\Delta_{31}|}{\sigma_1 + \sigma_3} \quad (9)$$

In which:

- σ_n represents the sigma parameter of the Gaussian distribution obtained when projecting the data points of group n in a 3 to 4 MHz range, which represents around 40% of all runs, on a vertical plane, as shown on Fig. 25;

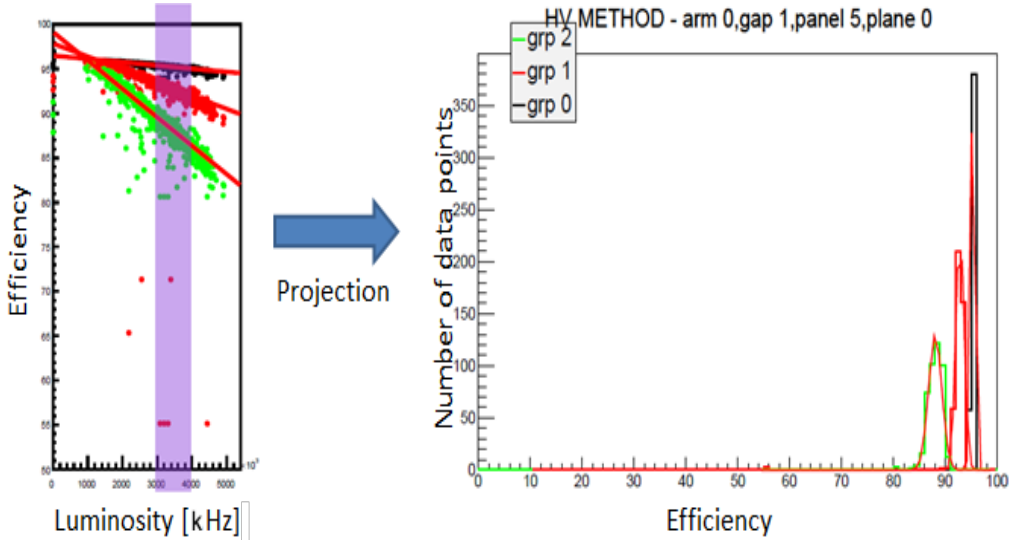

Fig. 22. Illustration of the principle of the evaluation of σ_n

- $|\Delta_{ij}|$ represents the distance between the fits of group i and group j at 3.5 MHz, as seen on Fig. 23.

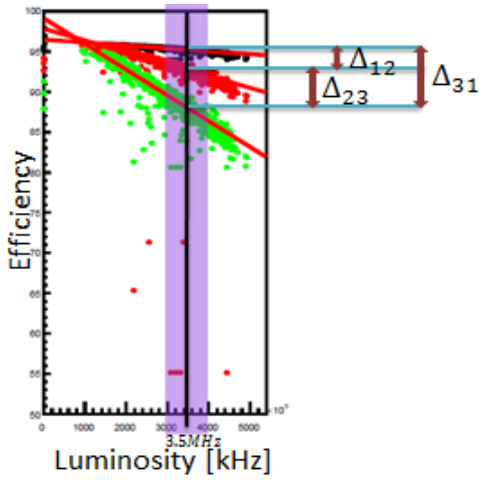

Fig. 23. Illustration of the principle of the evaluation of $|\Delta_{ij}|$

With such a definition, seriousness increases with growing $|\Delta_{ij}|$ and shrinks with σ_n, while giving an equal weight for all three groups.

I then used this weight to plot the histogram Fig. 24:

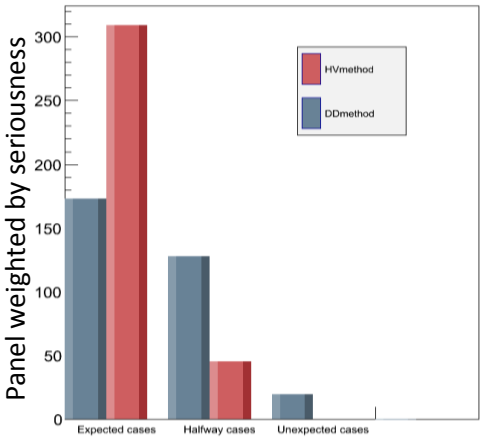

Fig. 24. Cases record of all gaps, weighted by seriousness

This histogram shows us that expected group orders have the largest occurrence, but that the occurrence of halfway cases isn't negligible.

c. <u>Incoming beam background</u>

As I searched for an explanation for these odd group orders, it has been suggested to me that they may be caused by particles incoming from the beam line. Indeed, though there is a shield to protect the detection layers from such particles, it is know that the upper parts of the last gaps of MuID suffer from higher hit rates due to this problem:

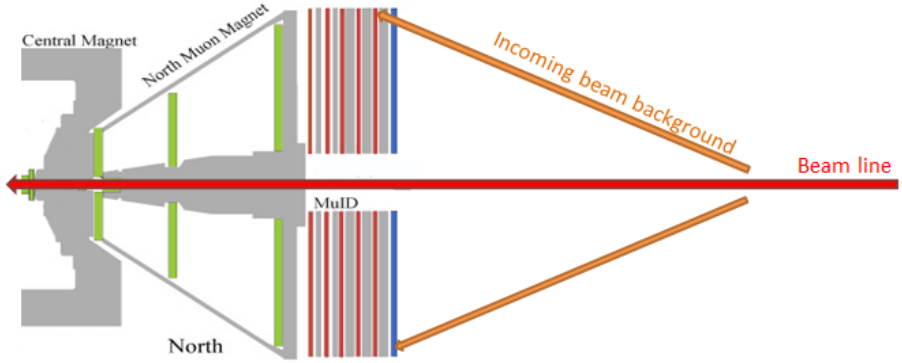

Fig. 25a. Incoming beam background

The hit rate record of this upper corner horizontal panel of Fig. 25b illustrates this quite well:

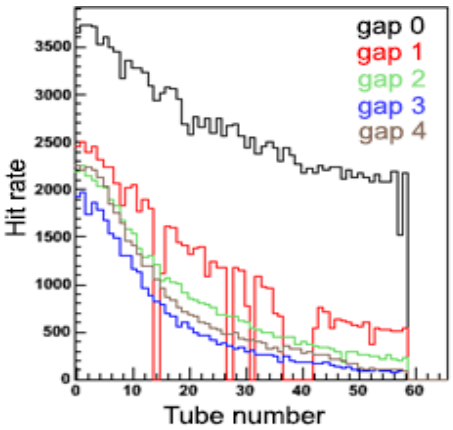

Fig. 25b. Hit rate record of North arm Horizontal panel 0

We expect the hit rates to decrease with the distance from the interaction point growing, meaning the hit rate from gap 0 should be higher than the hit rate from gap 1, and so on. However, the hit rate from gap 4, which is the furthest from the interaction point, is higher than gap 3 and even higher than gap 2 for the highest tubes.

Due to obvious geometrical reasons is mostly observable on horizontal planes: as it is shown on Fig. 26, all vertical groups receive the same amount of particles whereas this is not the case for horizontal ones.

Fig. 26. Incoming beam line particle problem illustration

With the knowledge of this problem, we plotted the same histogram as Fig. 24, but this time dividing it panel by panel and for both planes:

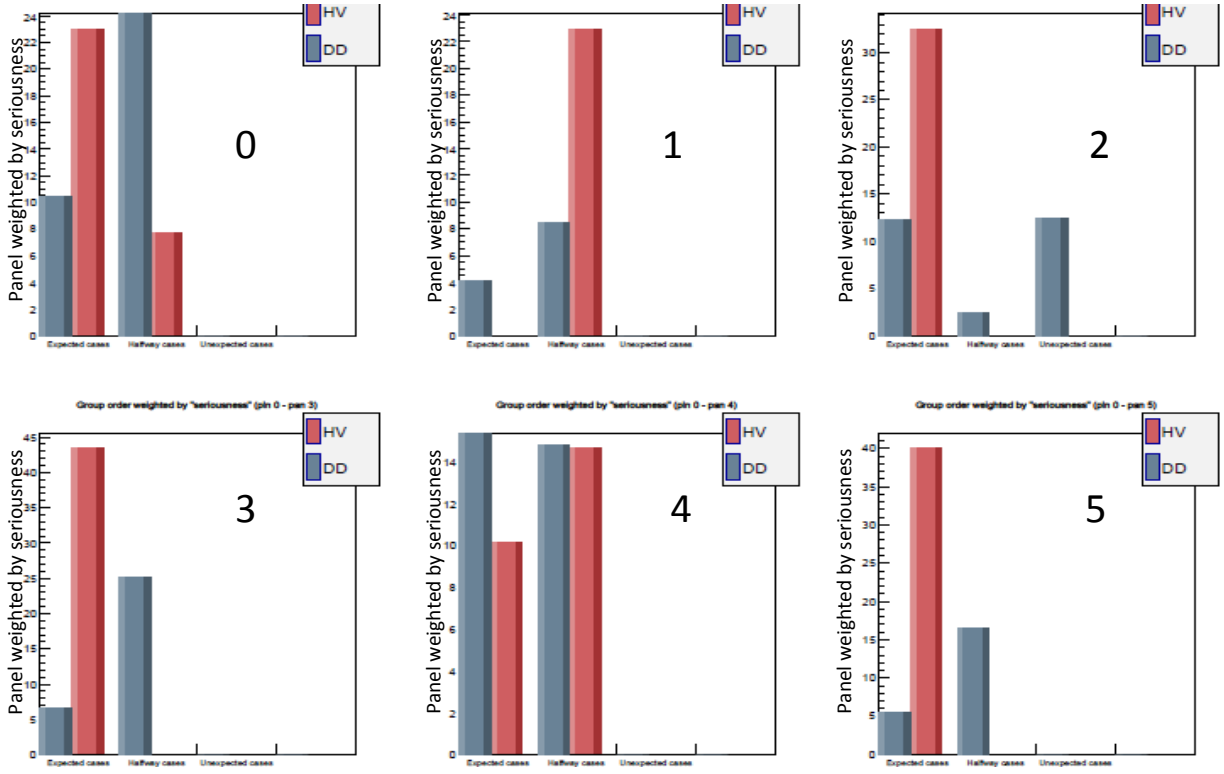

Fig. 27a. Panel-by-panel cases record, weighted by seriousness, for Horizontal plane

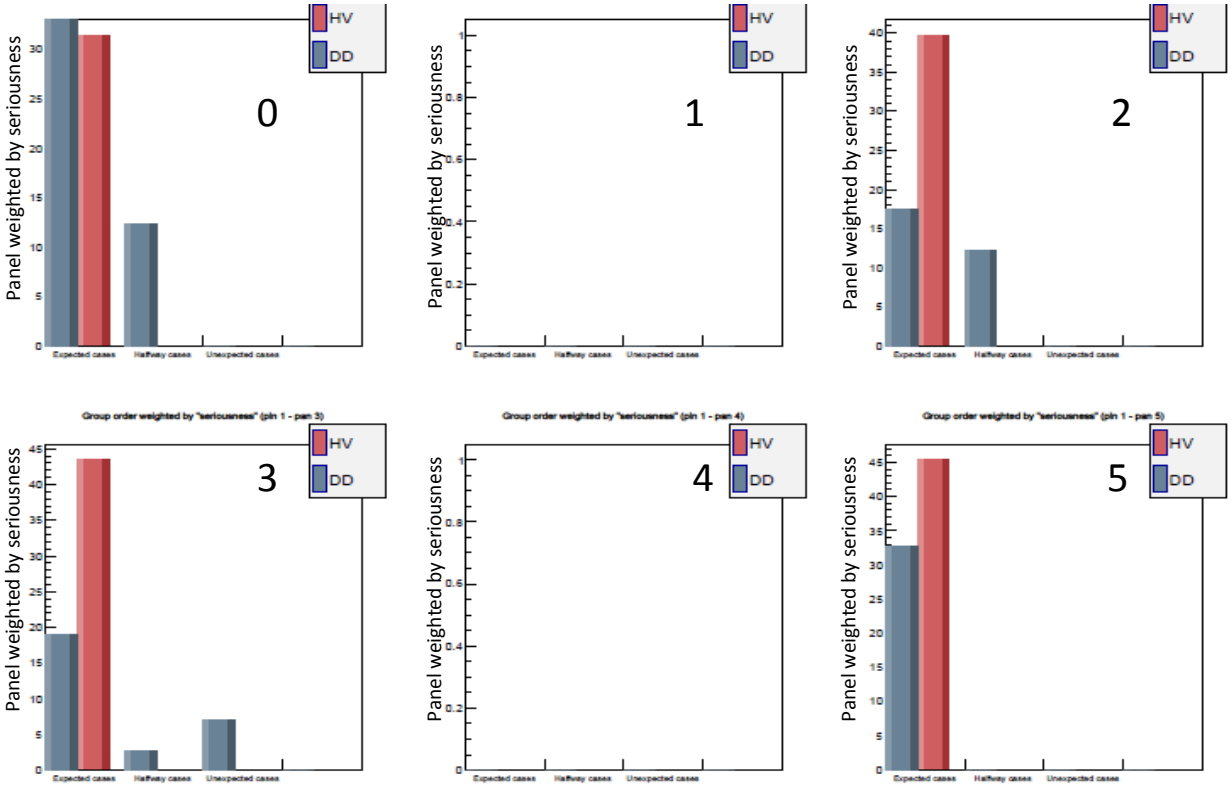

Fig. 27b. Panel-by-panel cases record, weighted by seriousness, for Vertical plane

As we can see by comparing Fig. 27a and 27b; the number of odd cases is indeed higher for horizontal panels, and there's also a higher proportion of odd cases on the upper part of MuID. Another observation we can make is that the proportion of odd cases is distributed differently for both methods, which hints at a geometrical bias for one of the two methods.

IV/ Correcting HV method

1/ New HV scan

a. 2014 HV scan

As it has been mentioned before the empirical formula (1), on which the whole HV method is based, was determined in 2004. PHENIX is now operating with higher luminosity than it used to, meaning that MuID is working with quite low efficiency conditions, where the relevance of the formula plays a rather crucial role. Knowing that, and with the possibility that MuID itself has been degraded over time, we took new data in July to verify whether or not this formula was still valid.

The aim of this HV scan, as it is called, was to get graphs similar to the ones presented in Fig. 9. The process consisted of a series of about a hundred cosmic runs where we would change the value of the HV supplies of each gap, one at a time, in order to simulate the voltage sagging induced by the high luminosity of physics runs. I then calculated the efficiency using the DD method, considered reliable for cosmic runs because we can assume that the data is taken at a 0 luminosity, meaning that there is no need to take into account the accidental coincidences that may occur with higher rates.

Fig. 28 shows the result of this HV scan for two different panels. The two behaviors shown here (one following the 2004 function, and the second one having a steeper curve) are the most common behaviors, and meet our expectations: either the detector shows the same response, or has been degraded over time.

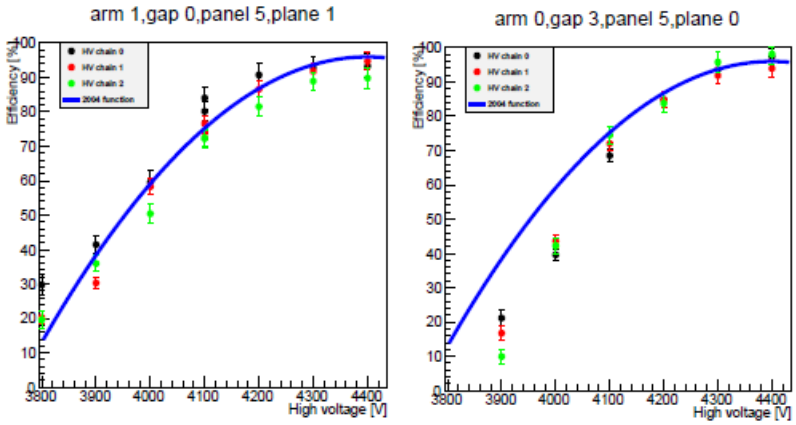

Fig. 28. Efficiency vs. HV – Expected behavior
Each color of data point represents a different HV group
Blue solid line represents the 2004 formula

However some of the panels from North arm show strange behaviors, as shown on Fig. 29, where the efficiency is constant through the whole scan. These behaviors may be due to a read-out problem, however this issue has not been solved yet and is still under investigation.

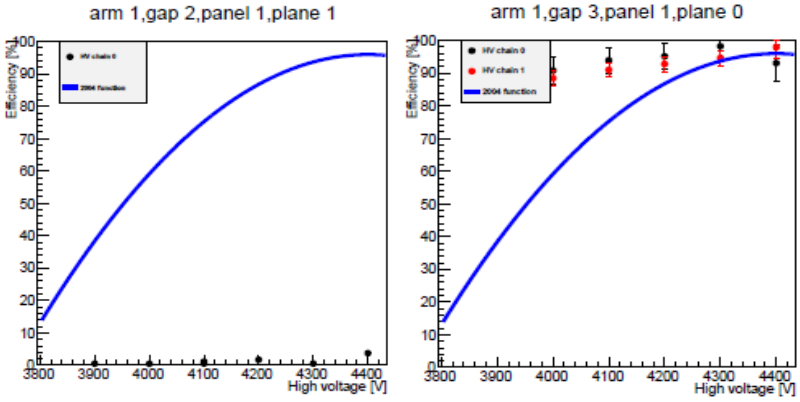

Fig. 29. Efficiency vs. HV – Odd behavior

With this set of data, the next step was to get a new fitting function for each HV group of MuID, regardless of the nature of the behavior. After trying different types of model functions, we finally kept the one based on the 2004 formula:

$$\boldsymbol{Efficiency = P_1(1 - P_2 \times V_{eff}^2)} \qquad (10)$$

In which $\mathbf{P_1}$ and $\mathbf{P_2}$ are the two fit parameters.

Results of this fit are shown for two typical panels in Fig. 30, each dotted line representing a fitting function:

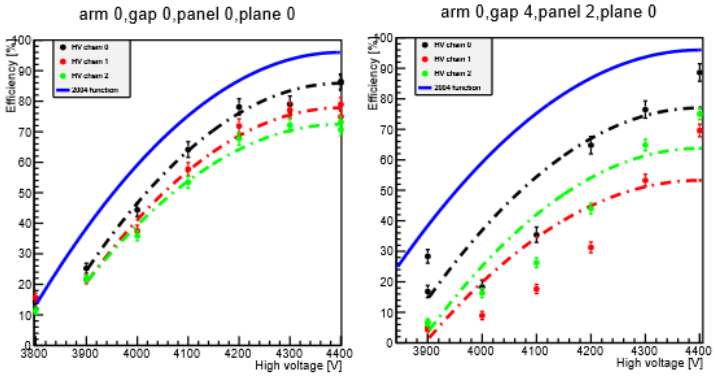

Fig. 30. HV scan fit – respectively good and poor fitting sample

As we wished for a more precise evaluation with the HV method, instead of averaging all functions into a single one, we kept them separated. I adapted my previous HV method program in order to use this new set of functions, and evaluated the efficiency of the physics runs with it.

b. <u>Comparing the new HV method results with the DD results</u>

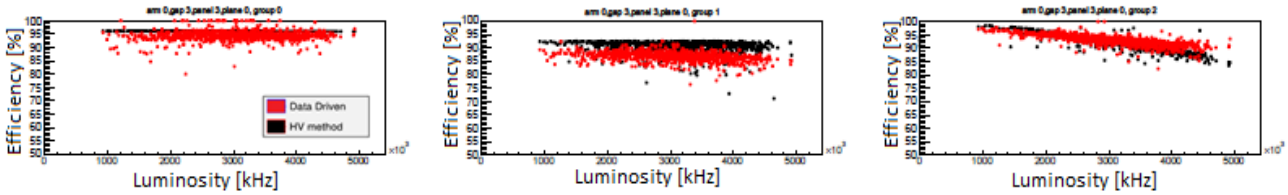

Fig. 31. Efficiency calculated with DD and new HV method for a particular panel
Every graph corresponds to a HV group
X axis is luminosity [kHz], and Y axis is efficiency [%]

Fig. 31 shows a comparison of the efficiency calculated with DD method and 2014 HV method for the same set of data. While for some groups there still is a clear discrepancy, the distributions show better agreement in most cases. The problematic groups can be correlated to the groups where the 2014 fit was not satisfactory.

In order to get a quantitative appreciation of the improvement brought by the 2014 HV scan, we can plot the average deviation plot with formula (8) once more:

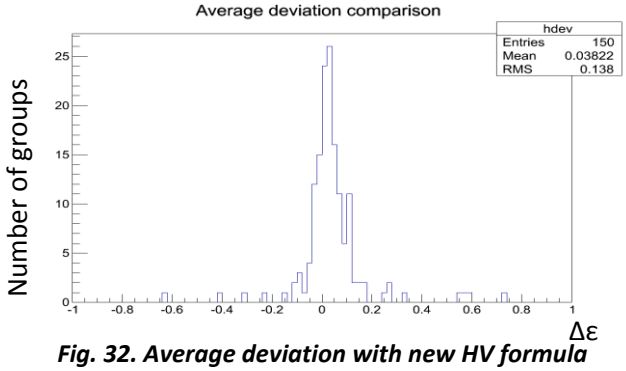

Fig. 32. Average deviation with new HV formula

Though the tendency of HV method to be higher than DD method is still present, the mean of the distribution has diminished from 8% to 4%. This means that though the 2014 HV scan was necessary to improve the HV method, it wasn't enough, hence the following correction.

c. DD method's bias

Thus far, I have proven that the efficiency calculated with the DD method is on average lower than the one calculated with HV method. However, both methods are inherently different by the way they are calculated.

One of the two major differences is the space difference: the efficiency of HV method relies on the current drawn by the entire length of the tube, meaning the efficiency is averaged over the whole tube; whereas the efficiency of DD method relies on tracks, and is therefore geometrically biased. In order to allow a fair comparison with HV method, we'll need to correct it with this geometrical bias.

Since the DD method is highly reliant on the tracks left on the panels, it is essential to get a better view of how they are distributed on MuID. As it has been mentioned before, the hit rate on MuID's gaps is higher around the beam line, and this can be visualized on Fig. 33 where each black dot represents a trace in the detector:

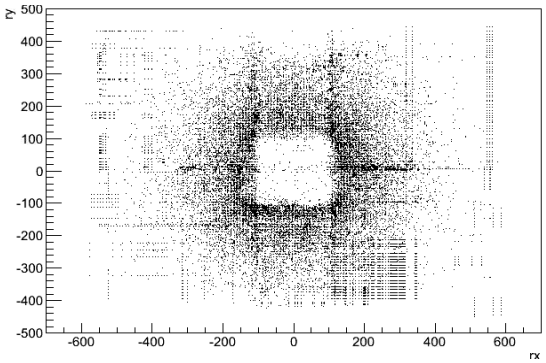

Fig. 33. Tracks recorded on all MuID's north gaps during part of a run

We can also see on this figure that the tracks are slightly higher on the edges of each panel, which allows us to see the shape of MuID. This is due to the fact that all panels slightly overlap each other in order not to lose any particles, resulting in a faintly better efficiency on these areas.

The first step of this analysis consists of dividing the previous plot into 4 different zones, as shown on Fig. 34, in order to get a quick estimation of the radius-to-the-beam-line-dependency of the efficiency calculated with the DD method.

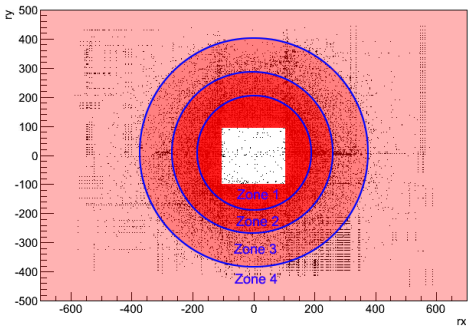

Fig. 34. Zone division of MuID

This was done by modifying the same pre-existing codes used for the evaluation of the efficiency through the DD method, this time creating a new division of the panels in these four zones. The results are presented on Fig. 35:

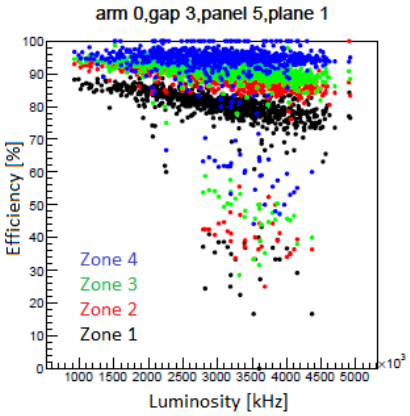

Fig. 35. Efficiency of a panel, divided into 4 zones

Fig. 35 points out the fact that the efficiency indeed depends on the radius to the beam line. And as expected, the zones with the least tracks density (i.e. zone 4) have the best efficiency.

In order to understand the nature of this dependency, we introduced an effective radius, $\mathbf{R_i}$, evaluated as follows:

$$\mathrm{R_i} = \frac{\sum_{j=0}^{Nr} r_j \times T_j}{N_r \times T} \qquad (11)$$

In which $\mathbf{N_r}$ is the total number of runs between 3 and 4 MHz, $\mathbf{T_j}$ is the number of tracks for run **j**, T is the total number of tracks and $\mathbf{r_j}$ is defined as:

$$\mathbf{r_j} = \frac{\sum_{k=0}^{T_j} \rho_k}{T_j} \qquad (12)$$

Where $\boldsymbol{\rho_k}$ is the radius of the track **k**.

Results of this analysis is shown Fig. 36:

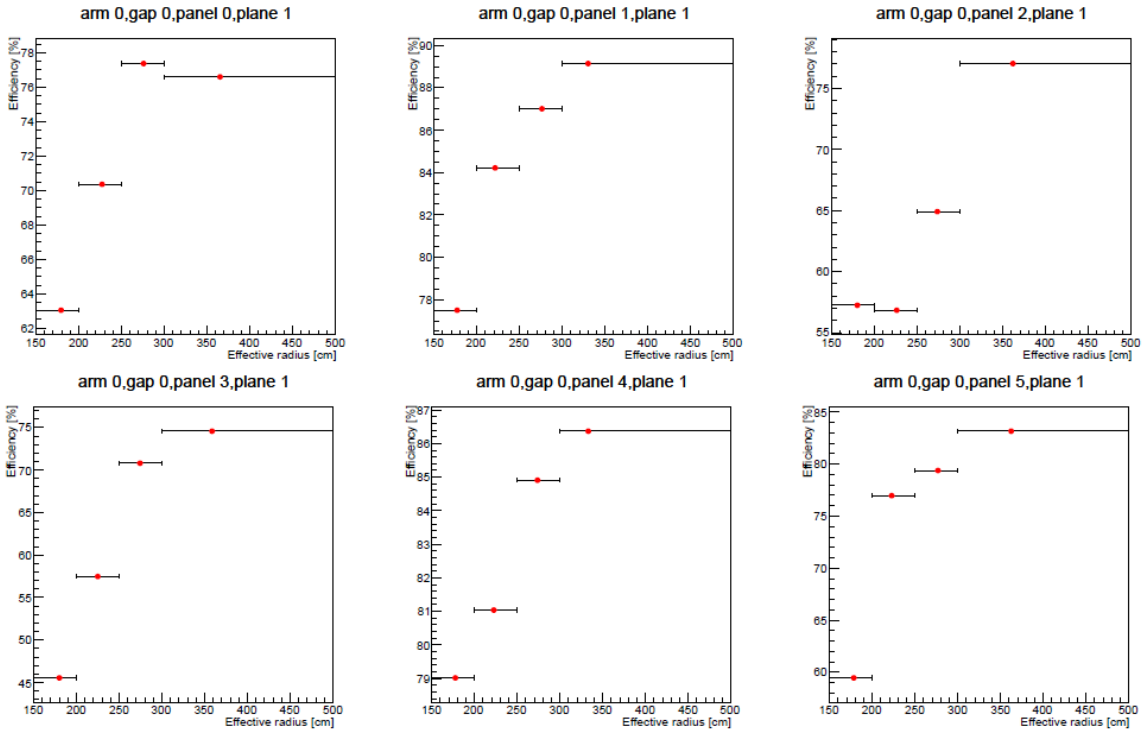

Fig. 36. Run-averaged plane efficiency vs. Effective radius for a particular plane

On these plots, it is clear that the efficiency is strongly radius-dependent and that it drastically drops near the beam line.

This result is not only relevant to the correction of the HV method, and actually raises a problem for other physics studies, especially for the calculation of cross sections involving the W boson which are produced with very specific rapidities, **η**, a value proportional to the radius of a track .

These cross-section evaluations require an efficiency correction. However, as of now, the correction applied to the experimental results is based on a panel-averaged efficiency and do not take into account the radius dependency we just proved, which implies that this analysis may be of use to more than the updating of HV method.

In order to use the results of this analysis, the best way would be to find a model that fits all radius-dependency behaviors and that could be ported to other analysis programs. However, though it is not shown on Fig. 36, there is a wide variation of efficiency behaviors amongst the different panels, due to the efficiencies of the tubes that they consist of, that makes it difficult to fit with a single model.

To get a more precise idea of this complex behavior, we could increase the number of zone divisions and fit each panel with its own model, resulting in several models that could be used by other studies rather than a single one. However, as this matter was tackled at the end of my internship, I could not push the issue further.

Conclusion

I spent six months working on the analysis of MuID's efficiency, which gave me the opportunity to hone my root skills as well as my knowledge on collider's physics. Not only did I learn a lot in the sphere of what was useful for my analysis, but thanks to Dr. Nakagawa I also had the chance to expand my knowledge on the particles physics world.

The analysis I have been running since the beginning of March has progressed a lot. I was able to complete a program dedicated to the evaluation of MuID's efficiency through the HV method as well as a program that ran geometry consistency checks and a rough comparison for both methods. I could also participate in the evaluation of a new HV method formula, which resulted in an enhancement of its results. Lastly, I worked on DD method's geometry bias in order to further improve the HV method, and succeeded in pointing out a matter that could also affect other studies based on MuID.

The results of HV method are not yet satisfying yet: the issue of the geometry dependency is not entirely resolved, and the matter of the time dependency of DD method has not been tackled yet, however this analysis has definitely been a first step in the direction of improving the HV method.

BIBLIOGRAPHIC REFERENCES

[1] http://www.riken.jp/en/about/
[2] http://www.bnl.gov/about/
[3] http://www.bnl.gov/rhic/PHENIX.asp
[4] http://cerncourier.com/cws/article/cern/53091
[5] http://www-ist.cea.fr/publicea/exl-doc/201200005429.pdf
[6] http://www.phenix.bnl.gov/WWW/pub/phenixnim/e_muonarms/nim_4e_muon_arms.pdf
[7] http://www.phenix.bnl.gov/phenix/WWW/intro/detectors/focus/focus_muid.pdf
[8] V. Cianciolo *et al.*, Run-5 MUID Efficiency Results and Technical Details, PHENIX Analysis Note 501, 2006.

APPENDIX

1/ Impact of the changes brought by my HV method program

a. Calculation of baseline current

The difference in method, averaging and linear interpolation, has proved to affect the efficiency of forty-one out of the one hundred and fifty chains of MuID's South Arm. To quantify this difference, I used this definition of the deviation:

$$\Delta\varepsilon_i = \frac{\varepsilon_i^{Avg} - \varepsilon_i^{LI}}{\varepsilon_i^{Avg}} \qquad (13)$$

Thirty-five tubes out of the forty-one affected groups only show slight change in efficiency, as pointed out by the blue arrows on Fig. 37:

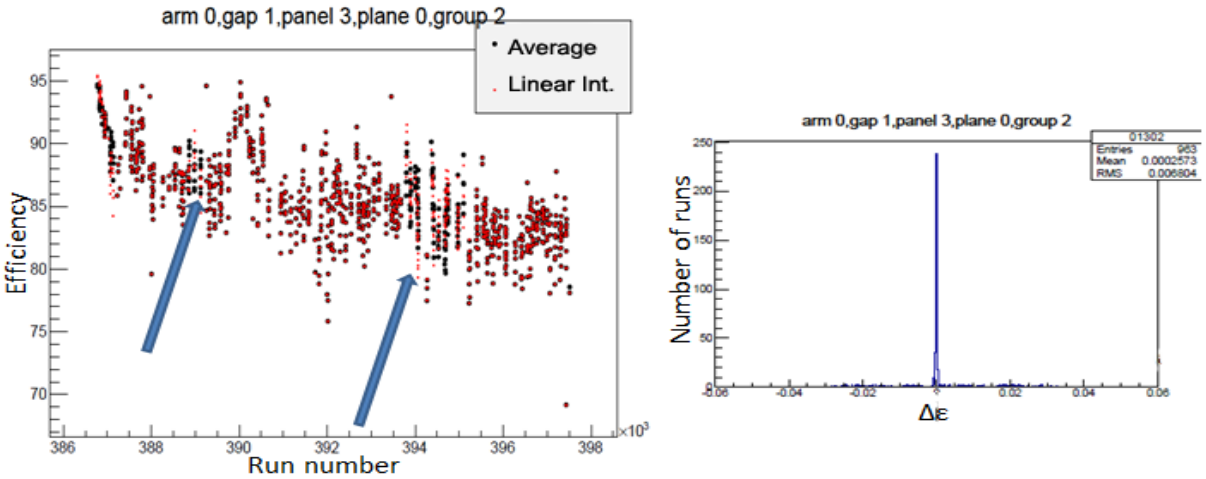

Fig. 37. Partial difference in efficiency between the two interpolation methods

In this case, the average deviation is largely below one percent.

Six out of the forty-one affected tubes show a change for almost all runs:

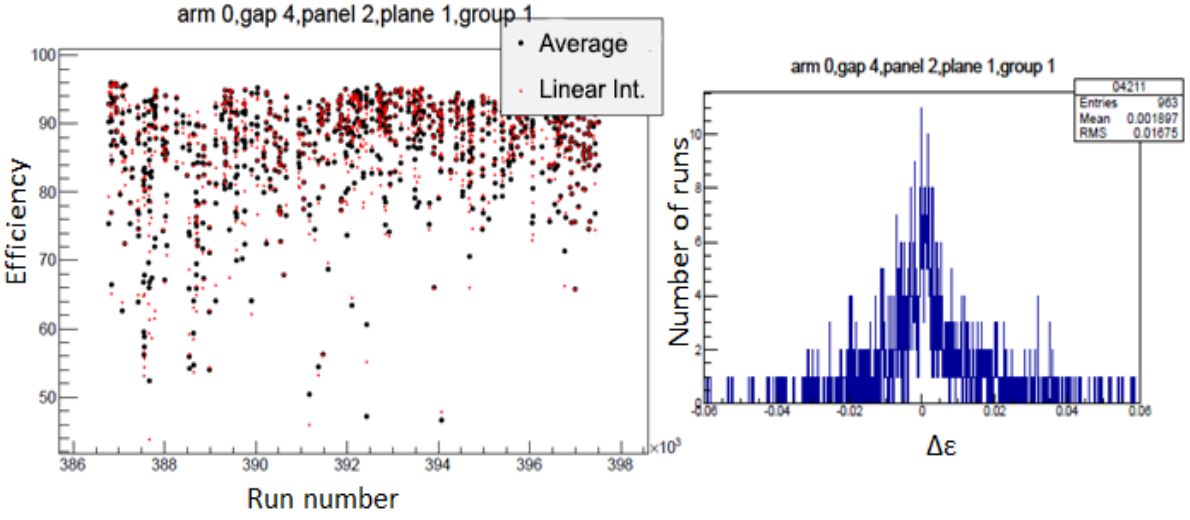

Fig. 38. Great difference in efficiency between the two interpolation methods

These six tubes were subject to great baseline current fluctuation, which explains how both interpolations gave results that differ on the whole physics run period.

In the worst cases though, the deviation between both methods is of only 5%. As we are not sure which of the two methods is more accurate as the moment, we have deemed that using any of the two was equally acceptable. Since it is part of my code, the rest of my analysis uses the linear interpolation method, but the final judgment is to be made by consistency check with DD method or to be included as systemic error of the HV method.

b. Evaluation of broken wires

The algorithm I programmed agreed with the previous visual determination for eleven out of the three-hundred wires. In most cases, the discrepancy occurred when the behavior of the baseline current was suspiciously unstable, such as the one Fig. 13.

I used the following definition to quantify the deviation in such cases:

$$\Delta\varepsilon_i = \frac{\varepsilon_i^{alg} - \varepsilon_i^{eye}}{\varepsilon_i^{alg}} \qquad (14)$$

This difference in method leads to a deviation that doesn't go over 5%, as seen on Fig. 19. As the algorithm I implemented in my program gives more reliable results than the human eye, we decided to keep it for the rest of the analysis.

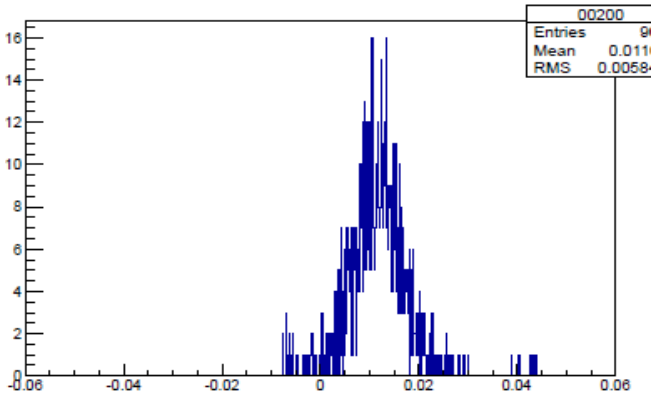

Fig. 19. Great difference in efficiency between the two broken wire determination methods

Abstract

This report summarizes my six-month long internship in RIKEN's Radiation Laboratory, located in Wako, Japan. This document includes a brief introduction to PHENIX and the MuID detector, then a detailed explanation of the process I used to evaluate MuID's efficiency, a comparison between both existing methods to calculate MuID's efficiency, an update on one of these two methods as well an introduction to the correction that will be applied to it.

Keywords

- Muon Identifier
- Efficiency evaluation
- Methods comparison

Résumé

Ce rapport résume mon stage de six mois au Radiation Laboratory de RIKEN, localisé à Wako, Japon. Ce document inclut une brève présentation de PHENIX et du détecteur MuID, puis une explication détaillée du procédé que j'ai utilisé afin de déterminer l'efficacité de MuID, une comparaison entre les deux méthodes existantes qui permettent de calculer l'efficacité de MuID, une amélioration de l'une de ces méthodes ainsi qu'une petite introduction aux corrections qui leur seront appliquées.

Mots clefs

- Muon Identifier
- Calcul d'efficacité
- Comparaison de méthodes